

## Correlation between thermal, optical and morphological properties of heterogeneous blends of poly(3-hexylthiophene) and thermoplastic polyurethane

This article has been downloaded from IOPscience. Please scroll down to see the full text article.

2006 J. Phys.: Condens. Matter 18 7529

(<http://iopscience.iop.org/0953-8984/18/32/002>)

View [the table of contents for this issue](#), or go to the [journal homepage](#) for more

Download details:

IP Address: 129.252.86.83

The article was downloaded on 28/05/2010 at 12:40

Please note that [terms and conditions apply](#).

## Correlation between thermal, optical and morphological properties of heterogeneous blends of poly(3-hexylthiophene) and thermoplastic polyurethane

Patrícia S O Patrício<sup>1</sup>, Hállen D R Calado<sup>1</sup>, Flávio A C de Oliveira<sup>2</sup>,  
Ariete Righi<sup>2</sup>, Bernardo R A Neves<sup>2</sup>, Glaura G Silva<sup>1</sup> and Luiz A Cury<sup>2,3</sup>

<sup>1</sup> Departamento de Química, Instituto de Ciências Exatas, Universidade Federal de Minas Gerais, CP 702, 30123-970, Belo Horizonte MG, Brazil

<sup>2</sup> Departamento de Física, Instituto de Ciências Exatas, Universidade Federal de Minas Gerais, CP 702, 30123-970, Belo Horizonte MG, Brazil

E-mail: [cury@fisica.ufmg.br](mailto:cury@fisica.ufmg.br)

Received 10 March 2006, in final form 29 May 2006

Published 25 July 2006

Online at [stacks.iop.org/JPhysCM/18/7529](http://stacks.iop.org/JPhysCM/18/7529)

### Abstract

A correlation between thermal, optical and morphological properties of self-sustained films formed from blends of poly(3-hexylthiophene) (P3HT) and thermoplastic polyurethane (TPU), with 1, 10 and 20 wt% of P3HT in TPU, is established. Images of scanning electron microscopy (SEM) show the formation of domains of P3HT into the TPU matrix, characterizing the blend material as heterogeneous. The heat capacity ( $C_p$ ) dependence on P3HT contents was investigated in a large temperature interval. In the region of the TPU glass transition, the difference between the experimental and predicted  $\Delta C_p$  values is more pronounced for the 1 wt% case, which strongly suggests that in this case there is a higher influence of the P3HT chains on the TPU matrix. The SEM images for the 1 wt% blended film present the formation of the smallest P3HT domains in the TPU matrix. The relatively high reduction of the PL intensity of the pure electronic transition peak in the 1 wt% blended film, in comparison to the other blended films and also to a pure P3HT film, favours the assumption that the smallest P3HT domains are at the origin of a more structural disordered character. This fact is in agreement with the results obtained by Raman spectroscopy and also by photoluminescence resolved by polarization in stretched self-sustained films, showing an ample correlation between morphological, thermal and optical properties of these blended materials. In addition, the thermoplastic properties

<sup>3</sup> Author to whom any correspondence should be addressed.

of the polyurethane configure very good conditions for tensile drawing of P3HT and other conjugated polymer molecules.

## 1. Introduction

Conjugated polymers are of increasing interest in fundamental studies for their optical [1–3], thermal [4–6], morphological [7, 8], structural [9] and transport properties [10–13], as well as their potential applications in organic electronic devices [14–17]. Although poly(*p*-phenylenevinylene) based materials are the most studied, the polythiophene family of conjugated polymers, in particular poly(3-hexylthiophene) (P3HT), has also received great attention due to the possibility of constructing organic field effect transistors (OFETs). P3HT OFETs have relatively high mobilities [10, 13, 18–20], reaching values from 0.01 to 0.2 cm<sup>2</sup> V<sup>-1</sup> s<sup>-1</sup>. The relatively high mobility of these structures is related to the structural order of the P3HT film induced by the regioregular head-to-tail coupling of the hexyl side chains. The degree of ordering (conformational and/or quasi-crystalline structure) can also be judged from the optical properties of the polymeric films (absorption and emission spectra), which in turn depend on the technique used to produce the film [21]. Films of higher ordering present a redshifted  $\pi$ - $\pi^*$  absorption (and/or emission) band, with well defined vibrational structure. From the structural point of view, polythiophenes can be synthesized with different side-groups, which can cause different chain packing in films [22–24]. Small side-groups, corresponding to smaller inter-chain distances, lead to a dense chain packing with the increase of inter-chain interaction via aggregate sites. As observed by Ruseckas *et al* [22–24], intra-chain excitons are efficiently trapped at aggregate sites, resulting in a relatively large redshift of the aggregate luminescence spectrum (sample with smaller inter-chain distances) in comparison to the intra-chain exciton spectrum (sample with larger inter-chain distances).

Polythiophenes have also been used to form blends with different types of regioregular poly(3-alkylthiophenes) [25] and other conjugated polymers [7, 26]. Blending polymeric materials is an attractive route to improve their properties and to provide wide applications. Thermoplastic polyurethane (TPU) is an interesting material to produce polymer blends, enabling us to combine its mechanical properties with the transport and optical properties of conjugated polymers.

In this work, thermal, morphological and optical properties of self-sustained films formed by blending P3HT with TPU at different concentrations of P3HT are investigated. Even though studies of polymer blends constitute a wide field of interest, only a few works treating blends of polythiophenes and polyurethane can be found in the literature [27, 28]. Moreover, to the best of our knowledge, the correlation of these different properties of P3HT/TPU blends has not been performed yet. The first goal is to achieve the optimal conditions to obtain a hostess matrix of TPU without interfering in the physical properties of the conjugated polymer P3HT. The thermoplastic properties of the polyurethane enabled the self-sustained P3HT/TPU films to be stretched in order to induce a higher chain alignment in the P3HT material. This is also an original idea when compared to other works [29–32], which have not used this stretching technique for tensile drawing of conjugated polymer molecules. The results show that P3HT/TPU self-sustained films are very stable and can be very useful to investigate transport and optical properties of the P3HT material. They are also suitable as a basic material to mould corrugated patterns in order to obtain a polymeric structure of distributed feedback lasers (DFBs) [33, 34] and other electro-optical devices. The paper is organized as follows: the synthesis of P3HT and TPU and the descriptions of the thermal, morphological and optical measurements are given in section 2; the analysis of the experimental results is presented in

section 3; finally, in the conclusions, the main results and the perspectives of the work are summarized.

## 2. Experimental details

### 2.1. Materials

Polyurethane was synthesized [35] by using MDI (4,4-diphenylmethane diisocyanate, Aldrich) and poly(tetramethyleneglycol) (Aldrich,  $M = 1000 \text{ g mol}^{-1}$ , supplier data) in DMF (N,N-dimethylformamide, Aldrich) under inert atmosphere. The average weight molar mass ( $\overline{M}_w$ ) obtained by GPC (gel permeation chromatography) with tetrahydrofuran (THF) as a solvent and polystyrene standards was  $100\,000 \text{ g mol}^{-1}$ , with a dispersion index of 1.3.

The polymerization of the regiochemical oxidized P3HT was adapted from procedures described elsewhere [36]. The monomer 3-hexylthiophene (0.05 M) was previously dissolved in chloroform. A suspension of  $\text{FeCl}_3$  (0.2 M) in chloroform of equal volume was carefully dropped into the monomer solution for 8 h, while being stirred at room temperature under a  $\text{N}_2$  atmosphere. After the addition was complete, the mixture was stirred for 16 h. The reaction mixture was poured into methanol, and a precipitate was formed. This precipitate was filtered off and washed with methanol several times. The low molecular weight and irregular part of the oxidized polymer was removed by Soxhlet extraction with methanol. The yield of polymer was 82%, and the weight was determined to be  $\overline{M}_w = 89\,000$  by GPC in THF with polystyrene standards.

The blends of P3HT with TPU were prepared by dissolving each component into THF solvent and subsequently stirring for 12 h. Three samples of P3HT/TPU (1, 10 and 20 wt% of P3HT in TPU) blend solution were prepared by mixing the appropriate amounts of the corresponding polymers. Self-sustained films were formed by casting the blend solution and drying under vacuum at room temperature for more than one week. The typical thickness of the self-sustained films was of the order of  $500 \mu\text{m}$ . SEM images of these films were obtained from a JEOL instrument, model 840A, for cryogenically fractured surfaces. Spin-casting films from each concentration were also prepared at 1500 rpm, inside a glove-box under inert atmosphere. The AFM images in these spin-casting samples were performed to have a basis of comparison and also to have another way to identify the blend constituent polymers. The atomic force microscopy (AFM) measurements were performed with a Nanoscope IV Multimode (Veeco Instruments) on intermittent contact mode using conventional silicon cantilevers. Phase contrast and topographic images were acquired simultaneously. Although phase images are not very sensitive to height differences, they are very sensitive to topographic features like borders and also to compositional differences, enabling the differentiation of polymers within the blend [37].

### 2.2. Thermal analysis

Temperature modulated differential scanning calorimetry (TMDSC) curves for P3HT and the three different concentration P3HT/TPU blends were obtained with a TA Instruments apparatus, model MTDSC 2920. In a TMDSC experiment, a sinusoidal modulation of temperature is superimposed on a linear temperature ramp with time. To better study the glass transition phenomena through TMDSC, it is useful to explore the 'in-phase' heat capacity ( $C_p$ ). It displays a sigmoidal change from glassy to liquid-like values at a temperature referred to as a 'dynamic' glass transition temperature [38]. Approximately 5 mg of each sample was loaded in an aluminium pan and the analysis follows the procedure of (a) ramp heating at  $20^\circ\text{C min}^{-1}$

up to 110 °C to dry residual volatiles, (b) isotherm for 1 min, (c) quenching (inside the DSC cell) with a rate of approximately 40 °C min<sup>-1</sup> down to -100 °C, (d) isotherm for 3 min, (e) modulation (amplitude of 0.5 °C min<sup>-1</sup> and 60 s period), (f) ramp heating at 3 °C min<sup>-1</sup> up to 200 °C (250 °C for PHT). Measurements were carried out using helium as a carrier gas, at a flow rate of 40 ml min<sup>-1</sup>. The same equipment was used to perform the standard DSC measurement of the oxidized P3HT powder in order to observe the melting behaviour. For this latest measurement, 5 mg of sample was heated at 10 °C min<sup>-1</sup>, from 30 to 275 °C, under helium atmosphere.

### 2.3. Photoluminescence and Raman spectroscopy

Photoluminescence (PL) spectra for the self-sustained P3HT/TPU films at the three different concentrations were measured at room temperature with the samples under vacuum, in order to avoid any photo-oxidation effect. A CW Ar-ion laser emitting at 514.5 nm was used as the excitation source. The PL emission was collected in a backscattering configuration, focused into a SPEX 0.75 m monochromator, and detected by a gallium arsenide (GaAs) photomultiplier tube.

In order to perform PL resolved by polarization, strips from each self-sustained film have been used. The stretched strips were kept under vacuum to avoid any photo-oxidation effect during the PL measurements. The stretching was performed at +45° from a vertical line (parallel to the slit of the spectrometer). The polarization of the excitation laser was maintained in the horizontal direction. The PL spectra were taken with the emission light passing through a polarizer parallel to the stretching direction (+45°) and also perpendicular to it (-45°). This set-up configuration enabled us to acquire the PL spectra avoiding losses of the optical system for a correct comparison of polarized spectra.

The Raman measurements of P3HT/TPU blends were performed in air in a Jobin-Yvon Raman system (model LABRAM 800) equipped with a cooled charge-coupled device detector. The spectra were collected in a backscattering configuration by a microscope using different (10×, 50× and 100×) objectives. The 632.8 nm line from a He-Ne laser was used as the excitation source.

## 3. Results and discussion

Results obtained from standard DSC and TMDSC techniques are shown in figures 1 and 2. Figure 1 presents the DSC heat flow for the P3HT powder in the melting region and the heat capacity ( $C_p$ ) curve for a P3HT casting film as a function of temperature. The  $C_p$  variation through the glass transition was obtained from the modulated experiment. In figure 2 are depicted the  $C_p$  versus temperature curves for TPU and the blends with 1, 10 and 20 wt% of P3HT in TPU. The curves in figures 1(b) and 2 present an anomalous feature between 30 and 50 °C, resulting from condensation in the measurement cell. This is a problem associated with our experimental set-up, and these anomalies have been discarded in the analysis.

P3HT is a semi-crystalline polymer which has been studied by several authors [39–43]. Figure 1(a) shows a large melting region from 120 to 240 °C with a peak at 216 °C and a total heat of melting of 14 J g<sup>-1</sup>. This behaviour is similar to that reported by Chen and Liao [39] for neutral P3HT and Hugger *et al* [43] for neutral and thin films of P3HT.

The onset temperature for the P3HT glass transition, determined from the  $C_p$  curve (figure 1(b)), is -10 °C as shown in table 1. Chen and Liao [39] by dynamic mechanical analysis (DMA) observed the backbone relaxation (or  $\alpha$ -relaxation) in the range -12 to 70 °C, which was assigned as the temperature range for the glass transition. From the  $C_p$  curve

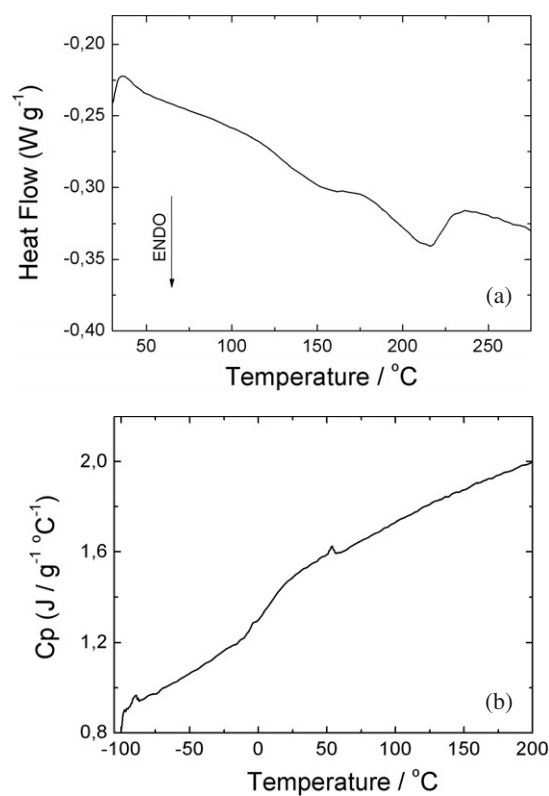


**Figure 1.** (a) Heat flow from standard DSC showing the melting region for oxidized P3HT powder; and (b) the heat capacity ( $C_p$ ) as a function of temperature for a P3HT casting film.

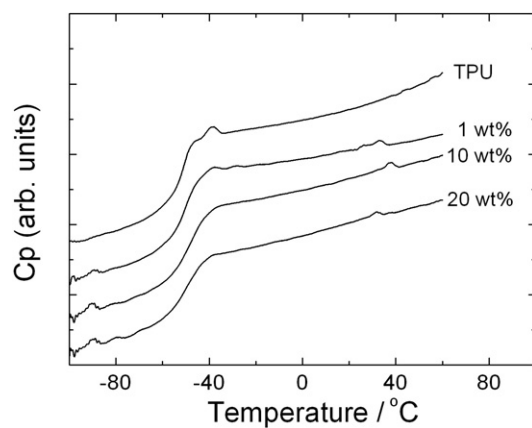


**Figure 2.** Heat capacity ( $C_p$ ) as a function of temperature for TPU and the blends with 1 wt%, 10 wt% and 20 wt% of P3HT in TPU.

(figure 1(b) and table 1), it is possible to associate the region from  $-10$  to  $22$  °C with the  $\alpha$ -relaxation of this polymer, according to [39]. The discrepancy in the temperature ranges comes from the different techniques, the different molar masses and also because we used oxidized

**Table 1.** TMDSC data for TPU, P3HT and P3HT/TPU blends in the glass transition ( $T_g$ ) region. ( $\Delta T_g = T_{g_{\text{endset}}} - T_{g_{\text{onset}}}$ .)

% in mass of PHT	$T_{g_{\text{onset}}}$ (°C) TPU phase	$\Delta T_g$ (°C)	$\Delta C_p$ (J g <sup>-1</sup> °C <sup>-1</sup> )	$\Delta C_p$ (J g <sup>-1</sup> °C <sup>-1</sup> )
				Calculated to the TPU phase <sup>a</sup>
0 (TPU)	-59	12	0.566	
1	-59	16	0.525	0.560
10	-57	17	0.505	0.509
20	-59	17	0.444	0.453
100	-10	32	0.293	

<sup>a</sup> Determined by taking the  $\Delta C_p$  value of the pure TPU (0.566 J g<sup>-1</sup> °C<sup>-1</sup>) and correcting by the mass of TPU in each blend.

P3HT material, while the P3HT sample of [39] is neutral. Zhao *et al* [41] and Hugger *et al* [43] determined, via the standard DSC technique, a temperature range for the glass transition between approximately -20 and 12 °C and between -16 and 8 °C, respectively. Considering the experimental differences between the TMDSC and the conventional DSC measurements of these last works [41, 43], one can affirm that there is a relatively good agreement between the glass transition data.

The glass transition corresponding to the P3HT phase was not detected in the  $C_p$  curves (figure 2) for the three blends studied. Taking into account the relatively low value of  $C_p$  variation ( $\Delta C_p$ ) for the P3HT during its glass transition, see table 1, and the relatively low concentrations of P3HT in the blends, there should be expected a very small signal compared to the higher variation of  $C_p$  for the TPU during the glass transition of the blends (figure 2 and table 1).

The comparison of the experimental  $\Delta C_p$  for the TPU phase in the blends with the values calculated from the pure TPU  $\Delta C_p$  and weighted by the amount of this material in each blend (table 1) shows a more significant difference for the 1 wt% case. This strongly suggests that there is a higher influence of the P3HT on the TPU matrix for the blend material at 1 wt%, even considering the low concentration.

The SEM and AFM images for the pure TPU and P3HT/TPU blends at concentrations of 1, 10 and 20 wt% of P3HT in TPU are shown in figures 3 and 4, respectively. From the SEM image in figure 3(a) the TPU surface is homogeneous and is characterized as a smooth fracture. For the blends in figures 3(b)–(d) the SEM images present heterogeneous morphology with different domains. The continuous phase, represented by the darker regions, is associated with the TPU matrix and the dispersive and spherical-like domains with the phase rich in P3HT. The quantity of the dispersive phase increases with the nominal P3HT concentration. The P3HT spherical-like domains, shown in figures 3(b)–(d), present different sizes, varying from 0.5 to 4.0  $\mu\text{m}$ . The smallest P3HT domains (0.5  $\mu\text{m}$ ) are seen in a bigger quantity for the case of 1 wt%. For the cases of 10 wt% and 20 wt% the domains present a more dispersed size distribution, not allowing a direct correlation between the P3HT concentration and the size of the domains.

AFM images of spin-casting films produced from the same solutions as the self-sustained films were taken in order to complement the SEM images. In the AFM topographic image of the pure TPU spin-cast sample—figure 4(a)—small protuberances are visible, which are a few nanometres high. However, the AFM phase contrast image of the same region—figure 4(b)—shows an almost constant phase shift, indicating a constant tip-sample interaction throughout this region [37]. Therefore, since a variation in sample composition would lead to a variation



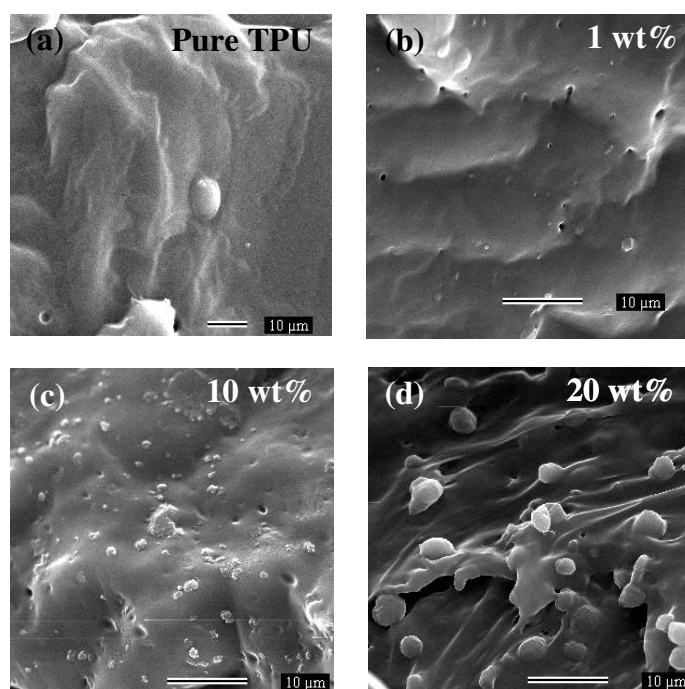


**Figure 3.** SEM images for (a) the pure TPU, (b) 1 wt%, (c) 10 wt% and (d) 20 wt% of P3HT in TPU. The bar at the bottom of each figure represents the size scale of the image.

in tip-sample interaction, figure 4(b) indicates a homogenous TPU surface [37]. In such a case, the small protuberances in figure 4(a) are probably formed by small air bubbles inside the TPU matrix (originated during solvent evaporation) or even small dust particles embedded by TPU. Therefore, the analysis of both figures 4(a) and (b) indicates that topographic AFM images can be misleading in the differentiation of polymer phases in a blend. As a consequence, phase contrast AFM images were employed to unambiguously reveal compositional variations in the blend, identifying its constituent polymers. Figures 4(c)–(h) correspond to the phase contrast AFM images and topographic AFM images of the blends with 1, 10 and 20 wt% of P3HT, respectively. Two different phases are clearly resolved in each phase contrast image: the TPU matrix (in grey) and P3HT circular domains (in white). It is also visible in the phase contrast images that the higher the P3HT concentration, the larger the circular domains. The ratio between the corresponding area for all circular domains and the corresponding area of the TPU for each concentration was determined. The obtained values are 1%, 10% and 19%, which are in very good agreement with the respective 1, 10 and 20 wt% of P3HT concentrations in the TPU matrix.

For the spin-cast films the size distribution of the P3HT circular domains depends on the P3HT concentration. Indeed, the mean diameter of the circular domains increases at higher concentrations. For 1 wt% of P3HT the diameter of the circular domains varies from 40 to 80 nm. For 10 and 20 wt% of P3HT the diameter ranges are 50–160 nm and 70–190 nm, respectively. In all cases the spin-cast films present much smaller P3HT domains in comparison to those observed from SEM images for self-sustained films.

The photoluminescence (PL) technique was used to study the emission properties of the P3HT/TPU self-sustained blend films. The typical PL spectra for the three self-sustained films



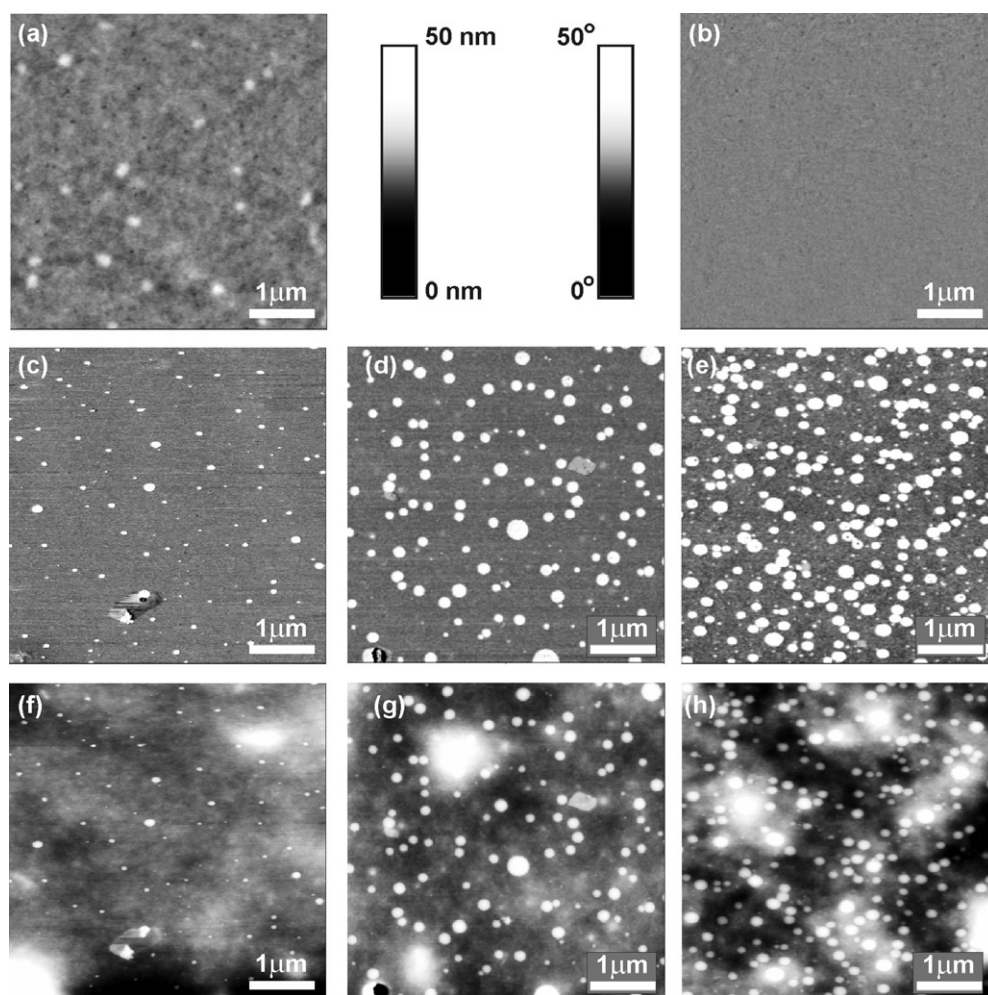


**Figure 4.** AFM images of pure TPU ((a) and (b)) and P3HT/TPU blends at concentrations of 1 wt% ((c) and (f)); 10 wt% ((d) and (g)); and 20 wt% ((e) and (h)) of P3HT in TPU. Parts (a), (f), (g) and (h) are topographic AFM images and the greyscale on the right side of (a) indicates the height of features in all these images. Parts (b)–(e) are phase-contrast AFM images and the greyscale on the left of (b) indicates the phase shift for all these images.

of blends and for the pure P3HT studied are shown in figure 5. The shoulder (00 transition) at around 550 nm was assigned to the pure electronic transition and the 01 peak at around 700 nm to the first vibronic band. The 00 shoulder almost disappears for the film with 1 wt% of P3HT, increasing with the P3HT concentration. The first vibronic band also displaces to higher wavelengths with increasing P3HT concentration.

The smaller the P3HT phase domain, the higher the influence imposed by the TPU matrix on the P3HT chains. This could lead to an enhancement of the structural disorder of the P3HT guest polymer, which is expected to be more relevant in the case of 1 wt% P3HT concentration with a larger number of small ( $0.5 \mu\text{m}$ ) domains. Higher structural disorder favours the decrease of the pure electronic 00 transition peak in relation to the vibronic bands [1, 44], which is in agreement with the very weak shoulder observed in figure 5 for the 1 wt% P3HT

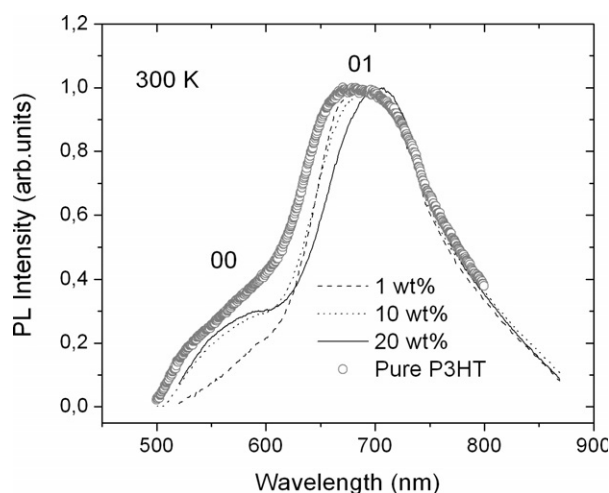


**Figure 5.** Photoluminescence spectra for a pure P3HT spin-cast film and for the self-sustained films with 1, 10 and 20 wt% of P3HT in TPU performed at 300 K. The spectra were normalized for a better comparison.

concentration. Different levels of structural disorder can also lead the  $\pi$ -electron to interact with different vibrational modes [45], changing the first vibronic band energy position. This could be a possible explanation for the displacement of the first vibronic band; however, more precise work is necessary to confirm this effect.

To complement the investigation of the optical properties of the P3HT/TPU blends Raman measurements have been performed. The Raman spectra taken at 300 K for the pure TPU and for the P3HT/TPU blends studied here are shown in figures 6(a) and (b), respectively.

The P3HT material absorbs very little laser light at 632.8 nm. However, it is enough to cause the appearance of a baseline in the Raman spectra due to the luminescence tail. This baseline increases with increasing P3HT concentration, which in part hides the Raman lines, making them appear smaller in intensity in the final corrected spectrum, as shown in figure 6(b).

The Raman spectra for the P3HT/TPU blends do not present any structure of the Raman spectrum from the pure TPU. This is probably because the excitation laser line (at 632.8 nm, used to acquire the Raman spectra) is close to the emission edge of the P3HT conjugated polymer, which characterizes a quasi-resonant condition with the consequence of increasing the P3HT Raman lines relative to those from TPU.

All Raman frequencies for the three blends in figure 6(b) are closer to those reported by Lefrant *et al* [9] in pure P3HT films. The band centred at  $1443\text{ cm}^{-1}$ , assigned to the C=C stretching, dominates the spectra, as has been also observed in other polythiophenic materials [46, 47]. The other Raman bands occur at 1378, 1208, 1181, 1167, 1088, 1000, 870, 725, 677 and  $596\text{ cm}^{-1}$ . The assignments for the majority of these bands are given in [9] and [48].

In figure 7 attention is focused on the behaviour of the bands at 725, 1167 and  $1181\text{ cm}^{-1}$ . The intensity of the band at  $725\text{ cm}^{-1}$  increases relative to the intensity of the band at  $1208\text{ cm}^{-1}$  and the shoulder around  $1170\text{ cm}^{-1}$  also evolves into two new bands at 1167 and  $1181\text{ cm}^{-1}$  with decreasing P3HT concentration. These bands, in particular, were observed by Lefrant *et al* [9] to increase due to oxidation, via doping of the P3HT macro-molecular chains with  $\text{FeCl}_4^-$ . These authors concluded that the changes in the profiles of the Raman lines were

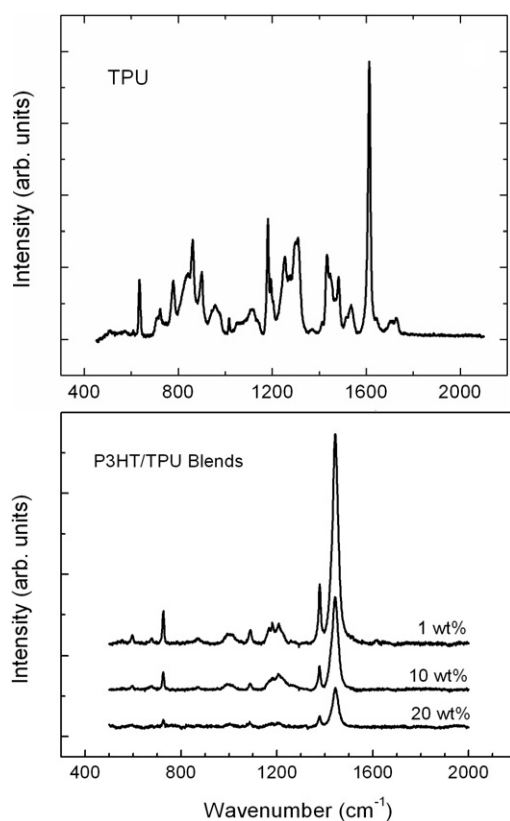


**Figure 6.** The Raman spectra at 300 K for (a) the pure TPU material and (b) 1, 10 and 20 wt% of P3HT in TPU blends.

due to structural disorder caused by steric effects induced during the doping process. According to the results of Lefrant *et al* the appearance of the bands at  $1167$  and  $1181\text{ cm}^{-1}$  and the relative increase of the band intensity at  $725\text{ cm}^{-1}$  were associated with a higher degree of disorder.

For the self-sustained films of P3HT/TPU blends the level of the structural disorder, probed by the optical properties, was dominated by the P3HT changes, mainly due to structural defects and/or intermolecular interactions inside the P3HT domains. Steric effects and/or interactions between the TPU and P3HT molecules at the interfaces of, and even inside, the P3HT domains can also contribute to changing the material structure. The observation of the 00 electronic shoulder in the pure P3HT spectrum (figure 5), with a relatively high intensity, but not in the spectrum of the 1 wt% blend, favours the assumption that the presence of the small P3HT domains is at the origin of the structural disordered character of the 1 wt% blended material. This fact also corroborates the changes observed in the Raman spectra (figure 7) for the three blended concentration samples. The clear PL reduction of the 00 shoulder at 1 wt% concentration (figure 5) is probably due to the contribution of the induced increase of chain defects and the P3HT–TPU steric effects at the interfaces of or inside the smallest P3HT domains.

In order to correlate the SEM and the TMDSC results with the optical properties of the blends, the self-sustained films were placed under different levels of stretching and studied via photoluminescence resolved by polarization. The behaviour of the integrated intensity ratio

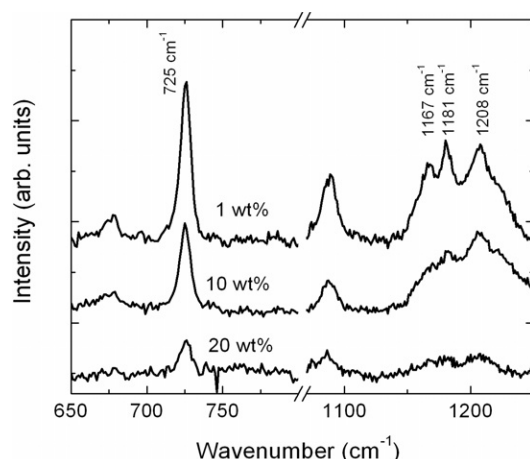


**Figure 7.** Enlarged view of Raman spectra focusing on the relative enhancement of the band at  $725\text{ cm}^{-1}$  and the appearance of the bands at  $1167$  and  $1181\text{ cm}^{-1}$ , for the blend with 1 wt% of P3HT in TPU.

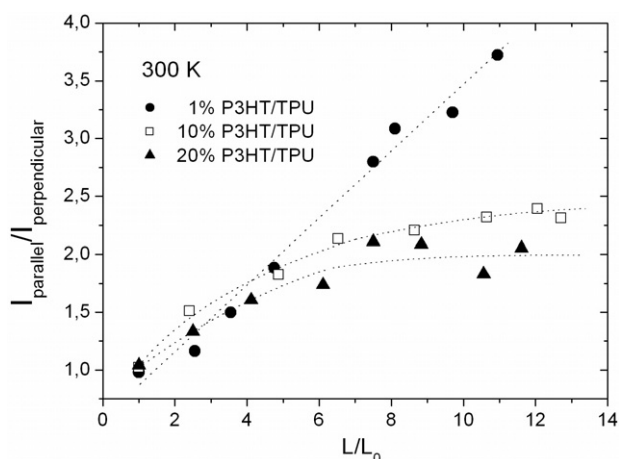


**Figure 8.** Ratio of the integrated intensity of parallel and perpendicular polarized PL spectra as a function of the stretching level ( $L/L_0$ ).  $L_0$  is the effective size of the initial stripe of the self-sustained films. The dashed lines are guides to the eyes.

of parallel and perpendicular polarized PL spectra with increasing stretching level is shown in figure 8 for the three blends in the study.

The integrated intensity rises faster for parallel emission than perpendicular in figure 8 or, in other words, the ratio  $I_{\text{parallel}}/I_{\text{perpendicular}}$  increases with stretching. Actually, it seems from the PL experimental results that the P3HT molecules are affected by the stretching procedure, showing a response which is associated with increase of conjugation or chain alignment in more organized structures, allowing a higher intensity of PL to be recorded in the parallel direction.

As observed from figure 8, the blend with 1 wt% of P3HT in TPU presents a linear behaviour of the integrated intensity ratio while the blends at higher concentrations tend to saturate, with a larger tendency for the case with 20 wt% of P3HT. Blends with 10 wt% and 20 wt% of P3HT have the largest domains. The adhesion of these domains depends on the

materials compatibility (interface interactions), the molecular weight of the chains [49], the rigidity and the level of stretching applied to the blend system. It can be proposed that phases forming larger domains are more susceptible to detaching from the TPU matrix under stress because they have fewer molecules per volume at the interfaces to interact in comparison with the materials with smaller domains. This assumption explains very well the PL results observed in figure 8, which shows the integrated intensity ratio saturation for the higher P3HT concentration blends.

#### 4. Conclusions

Self-sustained films of 1, 10 and 20 wt% of P3HT in TPU have been produced from the respective blend solutions in THF. They were studied by TMDSC, PL and Raman spectroscopy. The surface morphology of the films was analysed from SEM images. AFM images were also obtained for spin-casting films with the same concentrations for the sake of comparison and also to have another way to identify the blend constituent polymers. The P3HT and TPU materials form a heterogeneous type blend with circular-like domains of P3HT guest material in the TPU matrix. The ratio between the P3HT domains and the TPU matrix obtained from the SEM and AFM images agrees with the nominal concentrations used. Any direct correlation of the size of the domains with the P3HT concentration was observed for self-sustained films, mainly in the cases of 10 wt% and 20 wt% concentrations. We have only observed that the smallest domains (0.5  $\mu\text{m}$ ) predominate for the self-sustained film with 1 wt% of P3HT concentration. Conversely, the domains in the spin-cast films are of the order of tens of nanometres, much smaller than the domains observed for the self-sustained films, and present a clear dependence on the P3HT concentration.

As we are dealing with heterogeneous blends, the P3HT domains in self-sustained films are susceptible to being detached from the TPU matrix, depending on the degree of interaction at the domain interfaces and the applied level of stretching. This effect was assigned to be the main reason for the saturation behaviour of the PL response observed for the 10 wt% and 20 wt% P3HT concentrations at figure 8, in contrast to the linear dependence on the stretching level ( $L/L_0$ ) observed for the 1 wt% case. This result placed the samples with 10 wt% and 20 wt% at practically the same optical and morphological conditions, regardless of their relative P3HT quantity. This is also observed in terms of the PL spectra of unstretched blends, where in both cases the 00 shoulder appears more prominently (figure 5) than the reduced 00 shoulder at 1 wt%. The same can be considered for the Raman results in figure 7, which corresponds to saying that the morphological and optical characteristics of the self-sustained films of P3HT/TPU are effectively correlated. The comparison of the experimental  $\Delta C_p$  with the estimated values shows a more significant difference for the 1 wt% case. This strongly suggests that in the case of 1 wt% there is a higher influence of the P3HT on the TPU matrix. This corroborates the PL results at figure 5 and completes the correlation of the thermal to the optical and morphological characteristics. Thus, the results presented in this work point out that P3HT/TPU blends with small content of P3HT are associated with a higher level of structural disorder, which is probably related to an increase of chain defects and intermolecular interactions at the interfaces of or inside the smallest corresponding domains.

We have shown that it is possible to obtain a blended system of P3HT in a TPU matrix without losing the main optical properties of pure P3HT. In addition, the P3HT/TPU self-sustained films presented a very good elastic property, enabling us to stretch them to at least five times the initial length of the strip for all P3HT concentrations used. All blends under stretching have presented relatively higher states of polarization for emitted light polarized in the stretching direction.

The combination of the elastic properties of TPU and the optical and electrical properties of P3HT in these blends makes them very suitable for electro-optical devices. Further works are being planned to investigate transport mechanisms under different levels of stretching of the blends. The correlation study of the optical and morphological properties of the spin-cast films used in this work is also under way.

### Acknowledgments

We thank CNPq, FAPEMIG and the Nanoscience Millennium Project for financial support. We also thank the Metallurgical Engineering Department of UFMG for permitting the use of its Raman facilities. Special thanks are addressed to Professor Luiz Orlando Ladeira, our colleague from the Physics Department, for fruitful discussions.

### References

- [1] Pichler K, Halliday D A, Bradley D D C, Burn P L, Friend R H and Holmes A B 1993 *J. Phys.: Condens. Matter* **5** 7155
- [2] Heunt S, Mahrt R F, Greiner A, Lemmer U, Bassler H, Halliday D A, Bradley D D C, Burn P L and Holmes A B 1993 *J. Phys.: Condens. Matter* **5** 247
- [3] Hagler T W, Pakbaz K, Voss K F and Heeger A J 1991 *Phys. Rev. B* **44** 8652
- [4] Ko S W, Jung B J, Ahn T and Shim H K 2002 *Macromolecules* **35** 6217
- [5] Wang H Q and Li X Y 2002 *J. Appl. Polym. Sci.* **86** 3316
- [6] Zheng M, Sarker A M, Gurel E E, Lathi P M and Karasz F E 2000 *Macromolecules* **33** 7426
- [7] Babel A and Jenekhe S A 2004 *Macromolecules* **37** 9835
- [8] Nguyen Thuc-Q, Yee R Y and Schwartz B J 2001 *J. Photochem. Photobiol.* **144** 21
- [9] Lefrant S, Baltog I, Lamy de la Chapelle M, Baibarac M, Louarn G, Journet C and Bernier P 1999 *Synth. Met.* **100** 13
- [10] Pandey S S, Nagamatsu S, Takashima W and Kaneto K 2000 *Japan. J. Phys.* **39** 6309
- [11] Sirringhaus H, Brown P J, Friend R H, Nielsen M M, Bechgaard K, Longeveld-Voss B M W, Spiering A J H, Janssen R A J, Meyer E W, Herwig P and de Leeuw D M 1999 *Nature* **401** 685
- [12] Ahlskog M and Reghu M 1998 *J. Phys.: Condens. Matter* **10** 833
- [13] Bao Z, Dodabalapur A and Lovinger A J 1996 *Appl. Phys. Lett.* **69** 4108
- [14] Reese C, Roberts M, Ling M and Bao Z 2004 *Mater. Today* **7** 20
- [15] Samuel D W and Turnbull G A 2004 *Mater. Today* **7** 28
- [16] Borchardt J K 2004 *Mater. Today* **7** 42
- [17] Braun D 2002 *Mater. Today* **5** 32
- [18] Majewski L A and Grell M 2005 *Synth. Met.* **151** 175
- [19] Wang G, Swensen J, Moses D and Heeger A J 2003 *J. Appl. Phys.* **93** 6137
- [20] Sirringhaus H, Tessler N and Friend R H 1998 *Nature* **280** 1741
- [21] Dicker G, Savenije T J, Huisman B-H, de Leeuw D M, de Haas M P and Warman J M 2003 *Synth. Met.* **137** 863
- [22] Ruseckas A, Namdas E B, Ganguly T, Theander M, Svensson M, Andersson M R, Inganäs O and Sundström V 2001 *J. Phys. Chem. B* **105** 7624
- [23] Ruseckas A, Namdas E B, Theander M, Svensson M, Yartsev A, Zigmantas D, Andersson M R, Inganäs O and Sundström V 2001 *J. Photochem. Photobiol. A* **144** 3
- [24] Ruseckas A, Namdas E B, Theander M, Svensson M, Yartsev A, Zigmantas D, Andersson M R, Inganäs O and Sundström V 2001 *Synth. Met.* **119** 603
- [25] Babel A and Jenekhe S A 2003 *J. Phys. Chem. B* **107** 1749
- [26] Babel A, Li D, Xia Y and Jenekhe S A 2005 *Macromolecules* **38** 4705
- [27] Njuguna J and Pielichowsky K 2004 *J. Mater. Sci.* **39** 4081
- [28] Liu M and Gregory R V 1995 *Synth. Met.* **69** 349  
Liu M and Gregory R V 1995 *Synth. Met.* **72** 45
- [29] Cao Y, Smith P and Heeger A J 1991 *Polymer* **32** 1210
- [30] Golodnistiky D, Livshits E, Ulus A, Barkay Z, Lapides I, Peled E, Chung S H and Greenbaum S 2001 *J. Phys. Chem. A* **105** 10098
- [31] Wegener M, Künstler W and Gerhard-Mulhaupt R 2004 *Integr. Ferroelectr.* **60** 111



- [32] Marletta A, Miwa R H, Cazati T, Guimarães F E G, Faria R M and Veríssimo-Alves M 2005 *Appl. Phys. Lett.* **86** 141907
- [33] Kallinger C, Hilmer M, Haugeneder A, Perner M, Spirkl W, Lemmer U, Feldmann J, Scherf U, Müllen K, Gombert A and Wittwer V 1998 *Adv. Mater.* **10** 920
- [34] McGehee M D, Diaz-Garcia M A, Hide F, Gupta R, Miller E K, Moses D and Heeger A J 1998 *Appl. Phys. Lett.* **72** 1536
- [35] Patrício P S O, de Sales J A, Silva G G, Windmöller D and Machado J C 2006 *J. Membr. Sci.* **271** 177
- [36] Andersson M R, Selse D, Berggren M, Jarvinen H, Hjertberg T, Inganäs O, Wennerström O and Österholm J-E 1994 *Macromolecules* **27** 6503
- [37] Magonov S N and Whangbo M-H 1996 *Surface Analysis with STM and AFM* (New York: VCH)
- [38] Hutchinson M and Montserrat S 2001 *Thermochim. Acta* **377** 63
- [39] Chen S-A and Liao C-S 1993 *Solid State Commun.* **87** 993
- [40] Van de Leur R H M, de Ruiter B and Breen J 1993 *Synth. Met.* **54** 203
- [41] Zhao Y, Yuan G, Roche P and Leclerc M 1995 *Polymer* **36** 2211
- [42] Malik S and Nandi A K 2002 *J. Polym. Sci. B* **40** 2073
- [43] Hugger S, Thomann R, Heinzl T and Thurn-Albrecht T 2004 *Colloid Polym. Sci.* **282** 932
- [44] Oliveira F A C, Cury L A, Righi A, Moreira R L, Guimarães P S S, Matinaga F M, Pimenta M A and Nogueira R A 2003 *J. Chem. Phys.* **119** 9777
- [45] Cury L A, Guimarães P S S, Moreira R L and Chacham H 2004 *J. Chem. Phys.* **121** 3836
- [46] Jin S and Xue G 1997 *Macromolecules* **30** 5753
- [47] Zerbi G, Radaelli R, Veronelli M, Brenna E, Sannicolò F and Zotti G 1993 *J. Chem. Phys.* **98** 4531
- [48] Trznadel M, Zagorska M, Lapkowski M, Louarn G, Lefrant S and Pron A 1996 *J. Chem. Soc. Faraday Trans.* **92** 1387
- [49] Hong B K and Jo W H 2000 *Polymer* **41** 2069